

C-C coupling on single-atom based heterogeneous catalyst

Xiaoyan Zhang, Zaicheng Sun, Bin Wang, Yu Tang, Luan Nguyen, Yuting Li, and Franklin (Feng) Tao

J. Am. Chem. Soc., **Just Accepted Manuscript** • DOI: 10.1021/jacs.7b09314 • Publication Date (Web): 20 Dec 2017

Downloaded from <http://pubs.acs.org> on December 20, 2017

Just Accepted

“Just Accepted” manuscripts have been peer-reviewed and accepted for publication. They are posted online prior to technical editing, formatting for publication and author proofing. The American Chemical Society provides “Just Accepted” as a free service to the research community to expedite the dissemination of scientific material as soon as possible after acceptance. “Just Accepted” manuscripts appear in full in PDF format accompanied by an HTML abstract. “Just Accepted” manuscripts have been fully peer reviewed, but should not be considered the official version of record. They are accessible to all readers and citable by the Digital Object Identifier (DOI®). “Just Accepted” is an optional service offered to authors. Therefore, the “Just Accepted” Web site may not include all articles that will be published in the journal. After a manuscript is technically edited and formatted, it will be removed from the “Just Accepted” Web site and published as an ASAP article. Note that technical editing may introduce minor changes to the manuscript text and/or graphics which could affect content, and all legal disclaimers and ethical guidelines that apply to the journal pertain. ACS cannot be held responsible for errors or consequences arising from the use of information contained in these “Just Accepted” manuscripts.



C-C coupling on single-atom based heterogeneous catalyst

Xiaoyan Zhang,^{abc} Zaicheng Sun,^b Bin Wang,^d Yu Tang,^a Luan Nguyen,^a Yuting Li,^a Franklin (Feng) Tao^{a*}

^aDepartment of Chemical Engineering and Department of Chemistry, University of Kansas, Lawrence, KS, 66045, USA

^bSchool of Chemistry, Beijing University of Technology, Beijing, 100080, China

^cState Key Laboratory of Photocatalysis on Energy and Environment and College of Chemistry, Fuzhou University, Fuzhou, 350116, China

^dSchool of Chemical, Biological and Materials Engineering, Oklahoma University, Norman, OK 73019, USA

KEYWORDS: Catalysis • C-C coupling • Single atom catalysis • Palladium

ABSTRACT: Compared to homogeneous catalysis, heterogeneous catalysis allows for ready separation of products from its catalyst and thus reuse of the catalyst. C-C coupling is typically performed on a molecular catalyst which is mixed with reactants in liquid phase during catalysis. This homogenous mixing at a molecular level in the same phase makes separation of the molecular catalyst extremely challenging and costly. Here we demonstrated that a TiO₂-based nanoparticle catalyst anchored singly dispersed Pd atoms (Pd₁/TiO₂) is selective and highly active for more than ten Sonogashira C-C coupling reactions (R≡H+R'-X→R≡-R'; X=Br, I; R'=Aryl or Vinyl). The coupling between iodobenzene and phenylacetylene on Pd₁/TiO₂ exhibits a turn-over rate of 51.0 diphenylacetylene molecules per anchored Pd atom per minute at 60 °C with a low apparent activation barrier of 28.9 kJ/mol and no cost of catalyst separation. DFT calculations suggest that the single Pd atom bonded to surface lattice oxygen atoms of TiO₂ acts as a site to dissociatively chemisorb iodobenzene to generate an intermediate, phenyl which then couples with phenylacetylenyl bound to a surface oxygen atom. This coupling of phenyl adsorbed on Pd, and phenylacetylenyl bound to O_{ad} of TiO₂ forms the product molecule, diphenylacetylene.

INTRODUCTION

Carbon-carbon couplings including Suzuki, Heck, Sonogashira, Suzuki-Miyaura, and Stille C-C couplings have been considered as the cornerstones of organic synthesis.¹⁻²² For example, Suzuki-Miyaura cross-coupling of aryl halides with arylboronic acids has been the key step in production of arylalkynes and conjugated enynes which are important precursors for chemical production of industries.²⁻¹⁵ Typically, these C-C couplings use Pd(II) complex-based homogeneous catalysts such as Pd(PPh₃)₂Cl₂ (Figure 1a), called molecular catalysts. However, one obvious limit of using molecular catalysts is the technical challenge and quite high cost in separating a used molecular catalyst from the left reactants and formed products before reusing the catalyst or recycling the precious metal. Pd nanoparticles (NPs), a heterogeneous catalyst (Figure 1b) have been demonstrated to be active

for different C-C couplings^{3-7, 9-14, 16-19, 21, 23-24} in contrast to these conventional Pd-based molecular catalysts. Mechanistic understanding of C-C couplings on these heterogeneous catalysts, mainly Pd NPs protected with surfactant such as polyvinylpyrrolidone (PVP) or supported on metal oxide NPs is still an on-going topic.

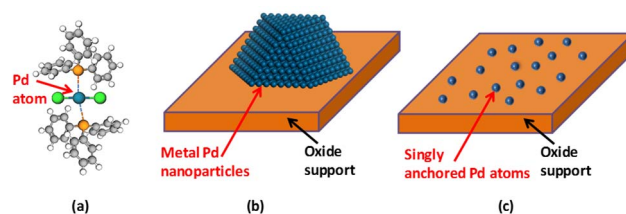


Figure 1. Schematic showing the structural models of Pd-based molecular catalyst (a) Pd(PPh₃)₂Cl₂, (b) Pd nanoparticle catalyst, and (c) Pd single atom catalyst (Pd₁/TiO₂).

Whether these metal nanoparticles are active phases of C-C coupling or not is still being debated.

As schematically shown in Figure 1b, metal atoms are continuously packed on surface of a metal nanoparticle. Atoms on a metal nanoparticle typically exhibits quite different coordination environments with their neighboring atoms. For instance, metal atoms at corners and edges have definitely different coordination numbers (CN) compared to those on facets.²⁵⁻²⁷ On the other hand, the fraction of atoms with a specific coordination number such as atoms at corners with CN (M-M)=7 strongly depends on size and shape of metal nanoparticles. Size- and shape-dependent catalytic performances on metal nanoparticles have been widely reported in literatures.²⁵⁻²⁷ Compared to the ubiquitous coexistence of multiple metal atoms with different coordination and chemical environments on surface of a metal nanoparticle (Figure 1b), a single atom of metal such as a Pd atom anchored on a nonmetallic substrate such as TiO₂ (Figure 1c) are expected to have a minimized number of choices of binding sites for reactants or intermediates. Thus, a catalyst with these singly dispersed metal atoms is expected to exhibit selectivity higher than a catalyst surface with multiple types of reactive sites such as Pd nanoparticles supported on TiO₂. More importantly, by anchoring precious metal atoms on a solid support, the catalyst can be readily separated. Such a catalyst is expected to exhibit high activity and selectivity and can be readily separated for reuse. Here we chosen the Sonogashira C-C cross-coupling of phenylacetylene and iodobenzene as a probe reaction and tested its activity and selectivity on Pd atoms singly anchored on TiO₂ toward both efficient catalysis and ready separation for high reusability of precious metals.

EXPERIMENTAL

Synthesis of catalyst. Pd(NO₃)₂·2H₂O (Aldrich) was used as the source of Pd cations for the preparation of singly dispersed Pd/TiO₂ catalyst. Anatase TiO₂ (99.7%, Aldrich) was used as the support. To anchor Pd cations. Catalyst precursors were synthesized through a deposition-precipitation method. In a typical preparation, 500 mg TiO₂ was mixed with 100 mL deionized water through a vigorous stirring to form a white suspension. 4.0 mL Pd(NO₃)₂·2H₂O aqueous solution (contain 2.6 mg Pd(NO₃)₂·2H₂O) was introduced to the TiO₂ suspension through controlled injection with a syringe pump while the solution was vigorously stirred. The new suspension was continuously stirred for 2-3 hrs to allow sufficient natural adsorption of metal ions. Then, the pH value of the mixture was carefully adjusted to 9.5 by gradually introducing ammonium hydroxide solution, followed by vigorously stirring for another 5 hrs in order to having a complete equilibrium in solution. Then the slurry was centrifuged and dried the solution at 60 °C in oven overnight; the catalyst precursor was calcinated at 400 °C in air for 4h. The catalyst was termed as 0.20 wt% Pd/TiO₂. The actual loading of Pd is 0.056 wt% based on inductively coupled plasma-atomic emission spectrometry (ICP-AES).

General procedure for performing Sonogashira C-C coupling on catalysts. Under nitrogen atmosphere, an oven-dried round-bottomed flask was charged with 0.20 wt% Pd/TiO₂ (50mg), K₂CO₃ (2.00 mmol), an aryl halide such as iodobenzene (1.00 mmol), a terminal alkyne such as phenylacetylene (1.00 mmol), 0.30 mmol dodecane and certain amount of ethanol, making the total volume of the

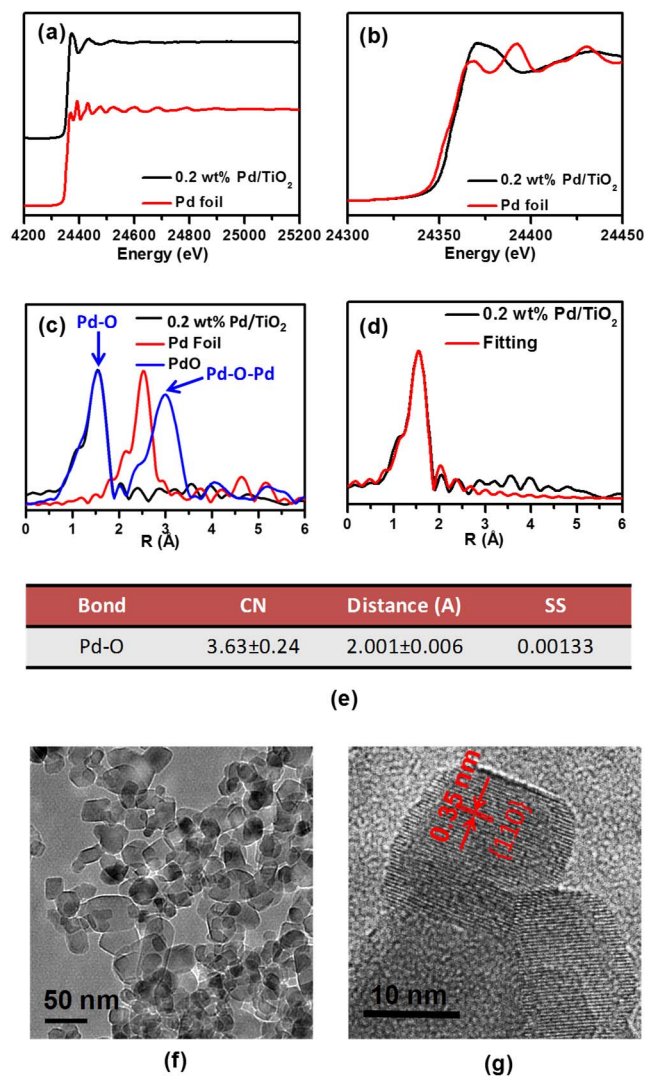


Figure 2. X-ray absorption fine structure of Pd K-edge and TEM studies of used 0.20 wt% Pd/TiO₂. (a) normalized absorption coefficient as the function of photon energy, (b) near edge absorption fine structure, (c) Fourier Transformed r-space data of the catalyst compared with Pd metal foil and PdO as references and (d) analysis and fitting of the r-space data of the 0.20 wt% Pd/TiO₂ catalyst, (e) fitting parameters of 0.20 wt% Pd/TiO₂ catalyst. The Pd foil and PdO reference are rescaled by the factors of 0.4 and 0.85 respectively for comparison in (c). (f) Large scale TEM image of catalyst particles. (g) High-resolution TEM of catalyst particles.

reaction mixture to 10.0 mL. All other substrates and corresponding catalytic performance can be found in Supporting Information. The catalysis was performed by heating the reaction mixture to 60 °C and then immediately stirring the solution vigorously at 60 °C for 3

hrs under the protection of nitrogen atmosphere. After fast cooling the refluxed solution to the room temperature with ice bath, the solution was centrifuged and filtered before GC-MS measurements of the amount of the format products and the amount of left reactants.

Measurements of formed products and left reactants. GC-MS is the main experimental technique to quantify the amounts of the left reactant and the formed products. Here the reaction system of C-C coupling between phenylacetylene and iodobenzene to form diphenylacetylene is used as one example to illustrate the method to quantify the reactants and products. The ideal product of this C-C coupling is diphenylacetylene. To accurately measure the amount of formed product and unreacted reactants for calculating conversion and selectivity of the C-C coupling, standard curves of the two reactants (iodobenzene and phenylacetylene) and the ideal product (diphenylacetylene) were established through preparing five solutions with different concentration for each of them. The relative intensity of GC peak of a reactant or a product to the added reference (0.30 mmol dodecane) was taken as Y-axis value in Figure S2. The corresponding amount of the chemical (iodobenzene, phenylacetylene, or diphenylacetylene) in unit of mmol was marked as the X-axis. By plotting this relative intensity in terms of area ratio of a chemical to 0.30 mmol dodecane as a function of the known amount of the chemical such as phenylacetylene, a linear regression was readily achieved as shown in Figure S2a. With the same method, the standard curves of iodobenzene and diphenylacetylene were established as shown in Figures S2b and S2c, respectively. They were used as standard curves in the calculations of conversions of iodobenzene, phenylacetylene and selectivity for production of diphenylacetylene.

Kinetic studies for C-C coupling on heterogeneous catalyst 0.20 wt% Pd/TiO₂ and homogeneous catalyst Pd(PPh₃)₂Cl₂. Under nitrogen atmosphere, an oven-dried round-bottomed flask was charged with 0.20 wt% Pd/ TiO₂ (5.0 mg), K₂CO₃ (2.0 mmol), iodobenzene (2.00 mmol), phenylacetylene (2.00 mmol), 0.30 mmol dodecane and ethanol, total volume of the solution is 10.0 ml. The reaction mixture was refluxed for one hour at different temperature (55 -75 °C). After cooling to the room temperature, the solution as centrifuged and filtered for GC-MS measurement.

Similarly, an oven-dried round-bottomed flask was charged with Pd(PPh₃)₂Cl₂ (0.50 mg), 99μl piperidine, iodobenzene (2.00 mmol), phenylacetylene (2.00 mmol), 0.30 mmol dodecane and acetonitrile, total volume of the solution is 10.0 mL. The reaction mixture was refluxed at a specific temperature under nitrogen atmosphere for 10 min. The kinetics of C-C coupling on Pd(PPh₃)₂Cl₂ was done in the temperature of 45-65 °C After cooling to room temperature, the solution was centrifuged and filtered for GC-MS measurement.

The reaction rate, r for C-C coupling on either 5.0 mg 0.20 wt% Pd/ TiO₂, or 0.50 mg Pd(PPh₃)₂Cl₂ was calculated with equation, $r = \frac{\text{transformed Iodobenzene (mol)}}{\text{Pd-based reactive sites (mol)} \times \text{reaction time in min}}$ when the catalysis was under kinetics controlled regime. The unit of r here is molecules of product per Pd site per min. In the kinetics studies, 2.00 mmol iodobenzene and 2.00 mol phenylacetylene were used as reactants; 5.0 mg 0.20 wt% Pd/TiO₂ or 1.0 mg Pd(PPh₃)₂Cl₂ (99%, Aldrich) was used as catalysts. The number of Pd-based sites of 5.0 mg 0.20 wt% Pd/TiO₂ was calculated to be about 1×10^{-7} mol. The number of Pd-based sites of 1.0 mg Pd(PPh₃)₂Cl₂ is 1.4×10^{-6} mol. For instance, the reaction rate on 0.20 wt% Pd/TiO₂ at 60 °C under kinetics controlled regime is 51.0 diphenylacetylene molecules produced from a Pd atom-based site per minute. It is 32.1 diphenylacetylene molecules produced from a Pd(PPh₃)₂Cl₂ molecule per minute at 60 °C under kinetics controlled regime.

Characterization. Powder X-ray diffraction patterns of the samples were measured on a Bruker SMART APEX single-crystal diffractometer. The size, shape and lattice fringe of the catalyst were identified using high-resolution JEM-2100F Transmission Electron Microscope operated at an accelerating voltage of 200 KV. X-ray photoelectron spectroscopy was conducted by using a lab-based ambient-pressure X-ray photoelectron spectroscopy system (AP-XPS) designed and built in Tao group. Amount of reactants or/and product in solutions before or after catalysis were analyzed with a GC-MS system containing GC (Quattro Micro) and mass spectrometer (LCT Premier) Samples are introduced into the Quattro Micro GC via the Agilent 6890N gas chromatograph equipped with an auto sampler; the LCT is equipped with a lock mass and is set to a resolution high enough to perform exact mass experiments when ions of the proper intensity are selected.

DFT calculation and optimization of TiO₂(101) surface. Density functional calculations were carried out using the VASP package²⁸. The Perdew-Burke-Ernzerh of generalized gradient approximation exchange-correlation potential (PBE-GGA)²⁹ was used, and the electron-core interactions were treated in the projector augmented wave (PAW) method³⁰⁻³¹. Structures were optimized until the atomic forces were smaller than 0.02 eV Å⁻¹ with a kinetic cut off energy of 300 eV. Van der Waals interactions were taken into account by incorporating the DFT-D₃ semi-empirical method³². Reaction barriers were determined with the Nudged Elastic Band method³³⁻³⁴. The optimized lattice constants of the anatase TiO₂ unit cell is 3.814 Å × 3.814 Å × 9.628 Å, which is in good agreement with experimental results³⁵. We modeled the TiO₂ (101) surface using a slab with four TiO₂ layers and a rectangular surface cell with dimensions of 20.7 Å × 19.1 Å. The vacuum layer is at least 16 Å in all the calculations to eliminate interactions between adjacent cells. The bottom 3 layers were fixed at their bulk positions while the top TiO₂ layer is fully relaxed.

RESULTS AND DISCUSSIONS

Formation single-atom catalytic site Pd₁O₄ on TiO₂.

The catalyst 0.20 wt% Pd/TiO₂ was synthesized through a well-controlled deposition-precipitation method with a following drying and calcination. The coordination environment of Pd atoms anchored on TiO₂ of a used 0.20 wt% Pd/TiO₂ was studied with X-ray absorption near edge structure (XANES) and extended X-ray absorption fine structure (EXAFS). Figures 2a and 2b present the energy space of Pd K-edge of both metallic Pd foil taken as a reference and the used 0.20 wt% Pd/TiO₂ after catalysis. Clearly, the edge position of Pd K-edge of the used 0.20 wt% Pd/TiO₂ in Figures 2a and 2b is different from metallic Pd foil. Compared to the Pd foil, the K-edge of Pd atoms in our catalyst has up-shift. It shows that the Pd atoms of our catalyst is at oxidizing state instead of the metallic state of Pd atoms of the Pd foil. Figure 2c presents *r*-space of Pd-K

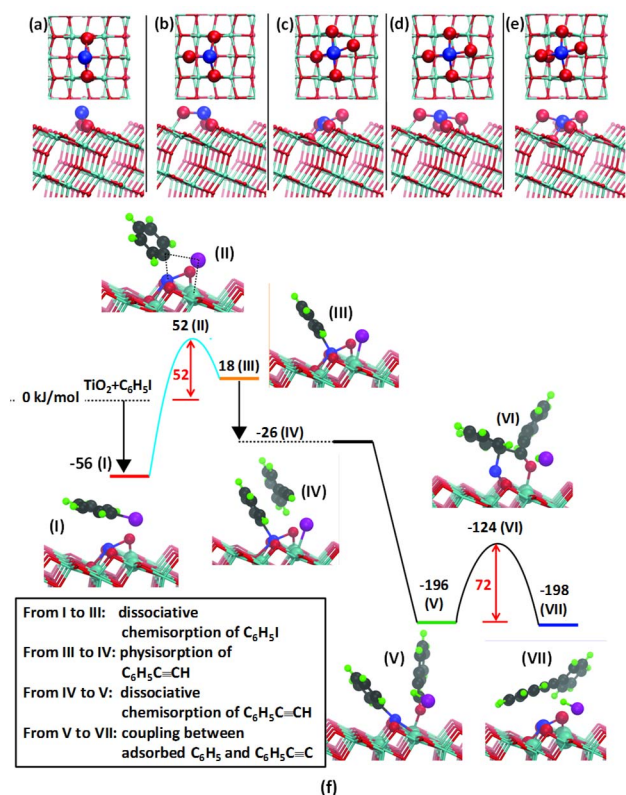


Figure 3. DFT calculations of the structures of the supported Pd₁ catalyst on anatase TiO₂ (101) surface and the reaction profile for the C-C coupling reaction. (a-e) five tested structures with varied coordination number and averaged Pd-O distance. (f) Reaction pathway proposed by DFT calculations and the corresponding energy profile. The Ti, O, Pd, C, H, I atoms are colored blue, red, blue, black, green, and pink, respectively.

edge of 0.20 wt% Pd/TiO₂ (black line), Pd foil (red line), and PdO nanocrystals (blue line). Obviously, the peak position of Pd K-edge of 0.20 wt% Pd/TiO₂ at ~ 1.45 Å in *r*-space is very different from the the Pd foil, showing the lack of metallic Pd nanoclusters in the used 0.20 wt% Pd/TiO₂. It does overlap the peak of the first shell of PdO, suggesting that Pd atoms of the used 0.20 wt% Pd/TiO₂ and PdO reference sample have a similar first coordination shell. The first shell of Pd K-edge of PdO was assigned to

Pd-O bond. Thus, these Pd atoms on the used 0.20 wt%

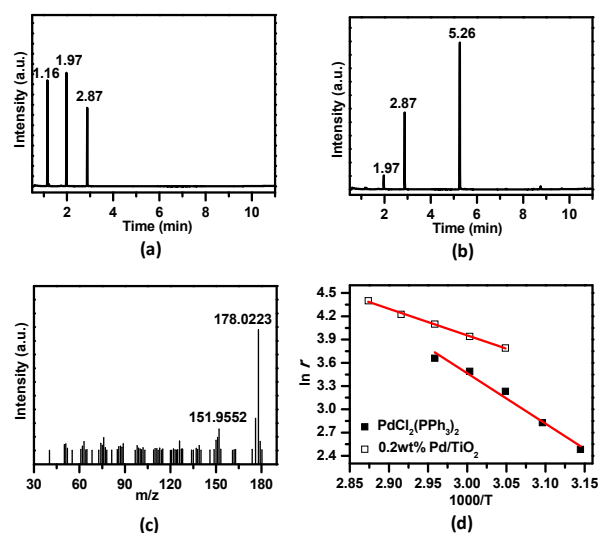


Figure 4. Catalytic performance of C-C coupling on Pd₁/TiO₂ and Pd(PPh₃)₂Cl₂. (a) GC spectra of reactants (phenylacetylene and iodobenzene) and internal standard (dodecane) before reaction. (b) GC spectra of solution after catalysis on 50 mg Pd₁/TiO₂, containing left reactants (phenylacetylene and iodobenzene), formed product (diphenylacetylene), and internal standard (dodecane); retention time for phenylacetylene, iodobenzene, dodecane, and diphenylacetylene is 1.16 min, 1.97 min, 2.87 min, and 5.26 min, respectively. (c) Mass spectrum of the product, diphenylacetylene separated by GC at 5.26 min. (d) Arrhenius plots of heterogeneous catalyst Pd₁/TiO₂ ($E_a=28.9$ KJ/mol) and homogeneous catalyst Pd(PPh₃)₂Cl₂ ($E_a=51.7$ KJ/mol); *r* is the reaction rate of phenylacetylene (molecule per Pd atom per min).

Pd/TiO₂ bonded with oxygen atoms of TiO₂. As shown in Figure 2c, PdO nanoparticles have very obvious second shell of Pd atoms in terms of Pd-O-Pd structure at 3.0 Å on *r*-space spectrum; the lack of this peak in the *r*-space spectrum of Pd K-edge of the used 0.20 wt% Pd/TiO₂ shows that our catalyst does not have Pd-O-Pd species. The lack of peaks of both Pd-Pd and Pd-O-Pd in *r*-space spectrum of the used 0.20 wt% Pd/TiO₂ shows Pd atoms of the used 0.20 wt% Pd/TiO₂ are obviously singly dispersed on surface of TiO₂ through bonding with oxygen atoms of TiO₂. Fitting the peak of the first shell of Pd-O (black line in Figure 2c) gives the average coordination number of oxygen atoms around a Pd atom, CN (Pd-O) = 3.63. It shows that on average each Pd atom bonds with about four oxygen atoms of the TiO₂ surface. The DFT calculations to be discussed later suggested that such a coordination in fact gives a stable structure as shown in Figure 3c. Pd₁/TiO₂ will be used to denote 0.20 wt% Pd/TiO₂ in some cases since we confirmed that Pd atoms are singly dispersed on TiO₂ through four Pd-O bonds. Morphology of the catalyst particles of Pd₁/TiO₂ were examined with TEM (Figure 2f). The average size of these nanoparticles is 20-25 nm. Lattice fringe of TiO₂ nanocrystals was measured. The

preferentially exposed surface of TiO₂ nanoparticles is (101) as shown in a representative image in Figure 2g.

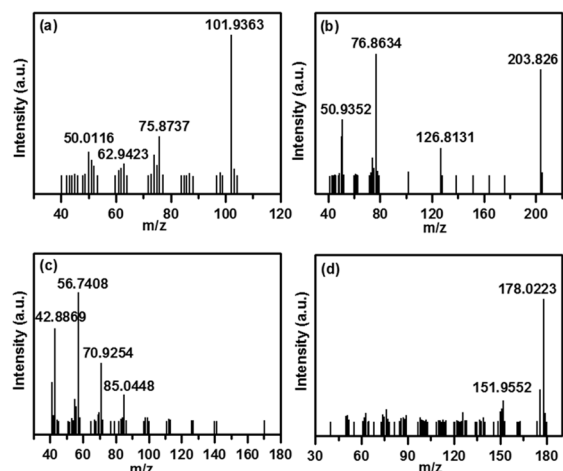


Figure 5. Mass Spectrum of (a) phenylacetylene, (b) iodobenzene, (c) dodecane, (d) diphenylacetylene separated by GC column as exemplified in Figures 4a and 4b.

GC-MS was used to separate different reactants in the solution before catalysis such as Figure 4a and separate reactants and products of a solution after catalysis such as Figure 4b. In GC of a solution before catalysis, the peaks at retention time at 1.16, 1.97, and 2.87 minutes are contributed from phenylacetylene, iodobenzene, and dodecane, respectively. In the GC of solution after catalysis on Pd₁/TiO₂, the peak intensity of phenylacetylene at 1.16 minutes attributed to phenylacetylene was below the detection limit, suggesting that most phenylacetylene was reacted. A new peak observed at 5.26 minutes is attributed to the product of diphenylacetylene. The recognition of a specific chemical (a reactant or product) in GC chromatography was clearly confirmed by its mass spectra in Figure 5. After reaction, the ratio of peak area of a reactant or product to the reference dodecane was calculated. For instance, with this ratio the amount of yield of diphenylacetylene after catalysis was readily calculated from Figure 5c.

The Sonogashira C-C coupling catalysis was performed at 60 °C for three hours. As shown in GC of the solution after catalysis (Figure 4b), no phenylacetylene was found. It shows phenylacetylene was completely transformed to products through C-C coupling on 50 mg 0.20 wt%

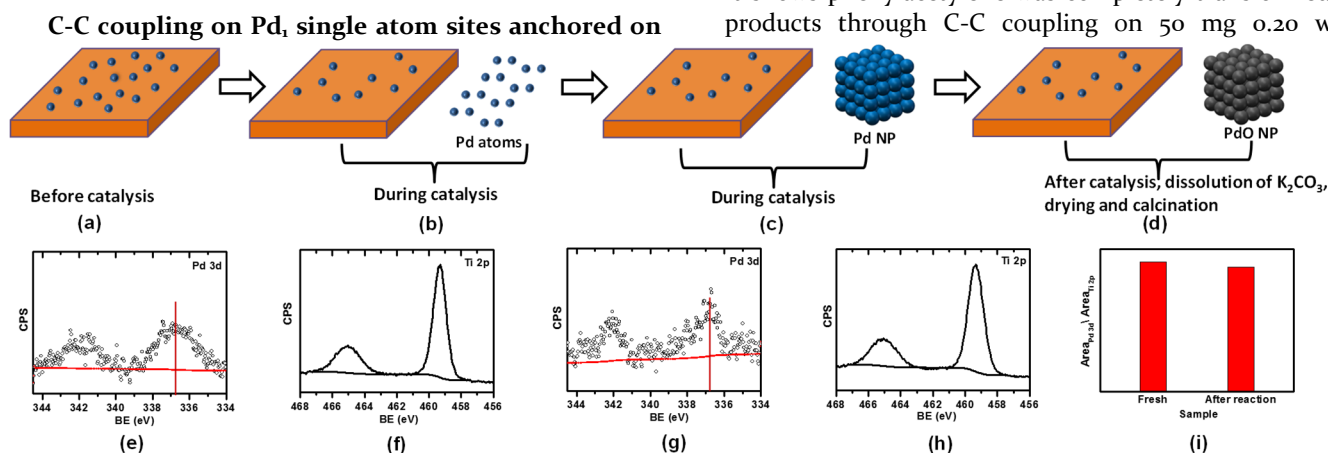


Figure 6. Control experiment for elucidating whether Pd atoms detached from surface of TiO₂ nanoparticles. (a) Schematic showing Pd₁/TiO₂ catalyst. (b) Schematic showing coexistence of Pd₁/TiO₂ and the detached Pd atoms during catalysis. (c) Schematic showing coexistence of Pd₁/TiO₂ nanoparticles and Pd nanocluster (after aggregation of Pd atoms) during catalysis. (d) Schematic showing coexistence of Pd₁/TiO₂ nanoparticles and PdO nanocluster formed drying solution containing calcinating Pd₁/TiO₂ nanoparticles and Pd nanocluster and then calcination in air. (e) XPS spectra of the Pd 3d of 0.20 wt% Pd/TiO₂ before catalysis. (f) Ti 2p of 0.2 wt% Pd/TiO₂ before catalysis. (g) XPS spectra of the Pd 3d of 0.20 wt% Pd/TiO₂ after catalysis, dissolution of base, drying and calcination. (h) XPS spectra of the Ti 2p of 0.20 wt% Pd/TiO₂ after catalysis, dissolution of base, drying and calcination. (i) Area ratio of peak of Pd 3d to peak of Ti of 0.20 wt% Pd/TiO₂ before catalysis (marked as “fresh” in the figure) and of 0.20 wt% Pd/TiO₂ after catalysis, dissolution of base, drying and calcination (marked as “after reaction” in the figure).

TiO₂. The catalyst was used for C-C coupling in a liquid phase which consists of 1.00 mmol iodobenzene and 1.00 mmol phenylacetylene as reactants, 2.0 mmol K₂CO₃ as a base, 0.30 mmol of dodecane, and certain volume of solvent (ethanol, dimethyl sulfoxide or benzene) which makes the total volume of the solution to 10.0 ml before catalysis. Dodecane is used as a reference for measurements of the concentrations of reactants and products with GC-MS. The details of measurements of product and reactants were described in experimental section.

Pd/TiO₂ and the conversion at 60 °C reached 99% under this catalytic condition. By calculating the area ratio of diphenylacetylene to dodecane and referring it to the standard curve of diphenylacetylene (Figure S2c), the yield of diphenylacetylene is >90%. Thus, the selectivity for production of diphenylacetylene is >91%. The reusability of the catalyst was tested by performing catalysis on the regenerated catalyst under a condition exactly same as the first cycle. The regeneration of the catalyst was done by drying the solution (after catalysis) in oven and then calcinating the powder in air at 500 °C for 4 hrs. The conversion of phenylacetylene and the selectivity for production of diphenylacetylene on the recycled catalysts

of the second and third cycles nearly remained little change as shown in Table S1. Thus, this catalyst exhibits the high activity, selectivity and reusability of 0.20 wt% Pd/TiO₂ for Sonogashira C-C coupling.

We performed that C-C coupling experiments on this catalyst by using seven aryl halides and three different terminal alkanes. The conversion and selectivity for C-C couplings of different substrates were listed in Table S2. As shown in Table S2, the catalyst Pd_i/TiO₂ exhibits high activity and selectivity for C-C couplings between Aryl halide (X=I and Br) and different terminal alkynes.

We tested the chlorobenzene with phenylacetylene and found that the activity for forming diphenylacetylene is low although couplings between terminal alkynes and bromobenzene and between terminal alkynes and iodobenzene on the Pd_i/TiO₂ catalyst are very active. The reason for the low catalytic activity of chlorobenzene is that C-Cl of chlorobenzene bond is stronger than C-Br of bromobenzene and C-I of iodobenzene. Thus, breaking C-Cl bond of chlorobenzene needs a higher temperature, leading to a low activity between chlorobenzene and terminal alkynes at 60-100°C. Notably, similar to the observed high activity for bromobenzene and iodobenzene and quite low activity for chlorobenzene, the quite low activity in C-C coupling between chlorobenzene and phenylacetylene on molecular catalysts was reported by Mery et al.³⁶ with the reported molecular catalyst, only 4% chlorobenzene can be converted although 100% iodobenzene can be converted under the same catalytic condition. A similar report on high activity on aryl halide (X=I and Br) and very low activity on aryl chloride (X-Cl) was published by Leadbeater et al.³⁷. Thus, the high activity of Pd_i/TiO₂ to these C-C coupling reactions between aryl halides (X=I and Br) and terminal alkynes clearly can justify that the Pd_i/TiO₂ is highly active for Sonogashira C-C coupling.

Catalyst with lower loading, 0.10 wt% Pd/TiO₂ was prepared with the same method as 0.20 wt% Pd/TiO₂. It shows low conversion (55%) but the same selectivity for C-C coupling. It suggests the sites on 0.10 wt% Pd/TiO₂ is very similar to 0.20 wt% Pd/TiO₂. In addition, 2.0 wt% Pd/TiO₂ was prepared as well. Catalysis on 2.0 wt% Pd/TiO₂ was performed under the same condition as 0.10 wt% Pd/TiO₂ and 0.20 wt% Pd/TiO₂. 50.0 mg catalyst of 2.0 wt% Pd/TiO₂ exhibits nearly 100% conversion but low selectivity of <75% due to the formation of Pd nanoparticles supported on TiO₂ nanoparticles.

Preservation of anchored Pd_i-based sites on TiO₂ during catalysis. One concern is that the activity of Pd_i/TiO₂ could have resulted from Pd nanoparticles if Pd cations could potentially detach from Pd_i/TiO₂ catalyst nanoparticles and then could have been reduced by ethanol to form Pd nanoparticles. It is reported that Pd nanoparticles are active for the C-C coupling although whether Pd nanoparticle is the active phase for C-C coupling or not has been debated.³⁸⁻⁴⁰ To explore the origin of the catalytic activity of Pd_i/TiO₂ catalyst, a key question is whether the Pd atoms of Pd_iO₄ sites anchored on TiO₂

could detach from Pd_i/TiO₂ during C-C coupling. To clarify it, we performed a few series of control experiments to check whether Pd nanoparticles formed or not.

A simple way to identify whether Pd atoms anchored on TiO₂ have been detached from surface of TiO₂ during C-C coupling, is to measure the concentrations of Ti and Pd in the liquid solution after precipitating the used catalyst nanoparticles Pd_i/TiO₂ by centrifugation. Here we call it *the simple method*. Through centrifuging the solution after catalysis, K₂CO₃ and the used catalyst were readily precipitated. Concentrations of Ti and Pd of the obtained solution after precipitation were measured with ICP-AES. Small portions of Pd and Ti atoms were found in the solution; the observation of Ti in the solution in fact results from the small TiO₂ nanoparticles of catalyst which could not be precipitated in the current centrifugation. About 7% of all Pd atoms of 50 mg 0.20 wt% Pd/TiO₂ catalyst remained in the solution after precipitation. Very likely, these Pd atoms detected by ICP after centrifugation are these Pd atoms anchored on these small catalyst nanoparticles (0.20 wt% Pd/TiO₂) whose sizes are too small to be centrifuged.

As mentioned above, if Pd cations could have detached from TiO₂ during catalysis, they should have been immediately reduced by the solvent such as ethanol to form Pd nanoparticles in the solution. This is because Pd²⁺ in solution can be immediately reduced by methanol at 25 °C to form Pd nanoparticles based on reference.⁴¹ To test the reducibility of ethanol to Pd²⁺, 1.0 μmol of Pd(NO₃)₂ (mass of Pd, about 1.0×10⁻⁴ gram) which is about 3.5 times of Pd cations of 50.0 mg of 0.20 wt% Pd/TiO₂ (about 2.8×10⁻⁵ gram of Pd) and the same amount of base 2.0 mmol K₂CO₃ were added to 9.8 ml ethanol at 25 °C, being a test solution. As shown in Figure S3a1, the solution was immediately turned to gray at 25 °C. It suggested the high reducibility of ethanol to Pd²⁺ at 25 °C. Upon the solution of Pd(NO₃)₂, ethanol and K₂CO₃ was heated to 60 °C and remained at this temperature, the color became dark. Figures S3a2-S3a4 show sequential change of color of the Pd(NO₃)₂ solution at 60 °C as a function of time. As reduction of Pd²⁺ of the Pd(NO₃)₂ solution to Pd atoms to form Pd nanoparticles is the only reduction reaction being performed in this test solution, the evolution of gray to dark of the test solution results from the formation of more Pd nanoparticles. The formation of Pd nanoparticles through reduction of Pd²⁺ by ethanol at room temperature were confirmed by TEM studies. An experiment using 0.28 μmol of Pd(NO₃)₂ (mass of Pd, about 2.8×10⁻⁵ gram) was performed under the same condition as the above experiment using 1.0 μmol of Pd(NO₃)₂; Similar to Figure S3a1, darkness of the solution at 25 °C was observed.

For comparison, the evolution of color of a typical catalysis solution was studied. The catalysis solution consisted of 50.0 mg catalyst nanoparticles 0.20 wt% Pd/TiO₂, 2.0 mmol K₂CO₃, 1.00 mmol phenylacetylene, 1.00 mmol iodobenzene, 0.30 mmol dodecane, and about 9.73 ml ethanol for making the total volume to 10.0 ml. Photos of the catalysis solution were taken at 0th hour at 25 °C, 1st hour at 60 °C, 2nd hour at 60 °C, and 3rd hour at 60 °C during catalysis (Figures S3b1-S3b4). At 25 °C, it was colorless

(Figure S3b1). Along the catalysis at 60°C, it turned to light yellow at 1st hour (Figure S3b2) and then orange at 2nd hour (Figure S3b3) and remained orange at 3rd hour (Figure S3b4). The evolution of color of the catalysis solution in Figures S3b1-S3b4 is distinctly different from the evolution of color of test solution consisting of 1.00 μmol Pd(NO₃)₂, 3.0 mmol K₂CO₃, and 10 ml ethanol in Figures S3a1-S3a4. TEM studies of the solution after C-C coupling catalysis of 3 hrs (Figure 3b4) showed that no Pd nanoparticles were formed in the solution during C-C coupling, consistent with the lack of dark color. This distinct difference of the two series of experiments in Figure S3a and S3b clearly suggest that the detected Pd in the solution after centrifuging the solution obtained after catalysis in *the simple method* was not in the format of free standing Pd cations since free standing Pd cations can be reduced to metal Pd atoms immediately even at 25 °C. Thus, the detected Pd atoms in ICP were the Pd atoms attached to small TiO₂ nanoparticles which cannot be centrifuged due to their small size.

Other than those control experiments, the following experiment was performed. 50 mg of 0.20 wt% Pd/TiO₂ was added to 10 ml ethanol; then was heat to 60°C and then remained at 60 °C under reflux condition; picture of the reaction system was taken at end of 1st, 2nd, and 3rd hour by quickly elevating the flask from oil heating bath to take a picture and then immediately putting it back to the 60 °C oil bath. As shown in Figure S3d1-S3d4, there is no change of the color of the solution. It is quite different from the obvious color change of 0.26 mg Pd(NO₃)₂·2H₂O in 10 ml ethanol (Figure S3a1-a4) and 0.026 mg Pd(NO₃)₂·2H₂O in 10 ml ethanol (Figure S3c1-c4). Thus, the lack of change of color of the solutions in the control experiment of Figure S3d1-d4 shows that the anchored Pd atoms on TiO₂ in ethanol of 3 hrs at 60 °C do not detach.

The preservation of anchored Pd atoms on 0.20 wt% Pd/TiO₂ nanoparticles left in solution in *the simple method* was further confirmed by XPS studies for measuring Pd/Ti atomic ratio of surfaces of fresh catalyst and used catalyst (Figures 6e and 6g). The 0.20 wt% Pd/TiO₂ nanoparticles left in solution was prepared by drying a mixture of ten experiments of *the simple method* through vaporizing water and solvent at 120 °C for 5 hrs. After drying, the left powder in beaker was collected and used as the sample of Figure 6g. XPS studies show Pd/Ti ratio of surface of the used catalyst remained the same as the fresh catalyst. The detailed description of this series of control experiments was provided in Section 1 of Supporting Information. Although the low signal to noise ratio of Pd 3d of the collected 0.20 wt% Pd/TiO₂ nanoparticles after drying (Figure 6g) makes the spectrum of Pd 3d in Figure 6g appear different from that before catalysis (Figure 6e), peak positions of Pd 3d_{5/2} in Figures 6e and 6g are the same. Thus, Pd atoms on TiO₂ before and after catalysis have very similar chemical state.

XPS cannot track the change of oxidation state of Pd atom in a catalytic cycle. In the case of homogeneous catalysis, the oxidation state does change from (0) to (II) when oxidative addition is performed in the first elementary step of a catalytic cycle; in the second step of

the catalytic cycle, it is reductive removal and Pd (II) is thus changed to Pd (0). As each catalytic cycle is performed fast, XPS cannot track the change of oxidation state of Pd atoms in a catalytic cycle. In the case of C-C coupling performed on surface of Pd₁/TiO₂, the formation of intermediate state (see structure III in Figure 3) can be considered as a step similar to oxidative addition of homogeneous catalysis; the bonding of a C atom of phenyl group to a Pd atom anchored on Pd₁O₄/TiO₂ should vary the electronic density; the desorption of diphenyl acetylene makes Pd atom of Pd₁O₄ restore to its original electronic state on TiO₂ and be ready for next catalytic cycle. These decrease of electron density of Pd atoms by bonding to carbon atom of phenyl and the increase of electron density by desorption of product molecule are performed in one catalytic cycle. As these elementary steps are performed fast; XPS cannot catch the change of oxidation state of Pd atom. Within one catalytic cycle, the binding of one C atom of a phenyl group to Pd atom changes the electronic state of Pd atoms; however, this change is not significant since Pd atom of Pd₁O₄ always bonds with four oxygen atoms of surface of TiO₂ nanoparticle. Photoelectron spectroscopy may not be able to identify this subtle change even if it could perform ultrafast scan at the timescale of finishing a catalytic cycle.

Another set of control experiments was performed to check whether the anchored Pd atoms on TiO₂ are active sites for C-C coupling at 60 °C. Different from all above series of catalysis reactions using ethanol as solvent, benzene instead of ethanol was used as a solvent in this series of control experiments. It is well known that benzene cannot reduce Pd cations to metallic Pd atoms to form Pd nanoparticles. Thus, the activity of 0.20 wt% Pd/TiO₂ in benzene must contribute from the anchored Pd atoms of 0.20 wt% Pd/TiO₂ if product molecules diphenylacetylene could be formed when benzene is used the solvent. The detailed description of this control experiment was given in Section 2 in Supporting Information. This control experiment showed that 50.0 mg 0.20 wt% Pd/TiO₂ is active for production of diphenylacetylene from C-C coupling of iodobenzene (1.0 mmol), phenylacetylene (1.0 mmol) at 60°C when benzene was used as the solvent. As benzene does not reduce Pd cations of 0.20 wt% Pd/TiO₂ to metallic Pd, the production of diphenylacetylene confirmed that the singly dispersed Pd atoms anchored on TiO₂ are intrinsically active for C-C coupling of iodobenzene and phenylacetylene.

Two hot filtration studies were performed. One was for measurement of the concentration of Pd atoms left in solution. In this study, C-C coupling between phenylacetylene and iodobenzene was performed at 60 °C for 1 hour and then immediately transferred the hot liquid to syringe filter to separate the reactant solution from the catalyst particles when the reaction system (the solution and the catalyst particles) was still hot. The Pd concentration of the filtered liquid was analyzed by ICP-AES. Upon removal of catalyst particles, the concentration of Pd in 10 ml solution (10.0 g) is 0.020 ppm; thus, the total amount of Pd in the solution is 2.0×10⁻⁷ gram. Compared to *the simple method* discussed early, much less Pd atoms

were left in the solution due to the use a fine filter paper in the syringe filtration. As mentioned in the preparation of catalysts of the experimental section, the actual concentration of 50 mg 0.20 wt% Pd/TiO₂ is 0.056 wt% Pd/TiO₂; thus, the total Pd in 50 mg 0.20 wt% Pd/TiO₂ is 2.8×10⁻⁵ gram. After reaction of one hour, 0.71% of all Pd atoms anchored on TiO₂ was detached. Similar studies were performed after catalysis of 3 hrs; the total amount of Pd in the solution is 0.57×10⁻⁶ gram after three hour reaction; 2.02% of all Pd atoms anchored on catalyst was detached.

Another hot filtration for checking whether Pd atoms detached from surface of TiO₂ or not was performed. After the hot filtration, the hot solution obtained after catalysis of 3 hrs was transferred back to a clean flask and 1.00 mmol iodobenzene and 1.00 mmol phenylacetylene, 2.0 mmol K₂CO₃ and 0.30 mmol dodecane were added to the solution; the solution was heat to 60 °C and remained at 60 °C for 3 hrs under reflux. After that, the solution was cooled to room temperature for GC-MS analysis. No detectable products were found in the GC-MS analysis. It shows that the contribution of Pd atoms left in the solution for the production of diphenyl acetylene is negligible.

Kinetics studies of C-C coupling on Pd_i/TiO₂ catalyst. Kinetics study of the C-C coupling on Pd_i/TiO₂ in the temperature range of 55 – 75 °C was studied in a kinetics controlled regime. Reaction rate, *r* was calculated by dividing the number of the reacted phenylacetylene molecules by the reaction time and the number of the Pd atoms anchored on TiO₂. By plotting **ln r** as a function of 1/*T*, an Arrhenius plot was achieved (Figure 4d). With the slope of Arrhenius plot, the apparent activation barrier for C-C coupling on 0.20 wt% Pd/TiO₂ was calculated. It is 28.9 kJ/mol. With the same method, the activation barrier of C-C coupling of phenylacetylene and iodobenzene by a molecular catalyst Pd(PPh₃)₂Cl₂ was measured in the temperature range, 45-65 °C. As shown in Figure 4d, the apparent activation barriers for the same C-C coupling catalyzed by Pd(PPh₃)₂Cl₂ is 51.7 kJ/mol.

Computational studies of C-C coupling on Pd_i/TiO₂. To understand catalytic mechanism of C-C coupling on Pd_i/TiO₂, we performed DFT calculations to optimize surface structure of Pd_i/TiO₂ and then simulate reaction pathway by using the anatase (101) surface which has a low formation energy. As shown in Figure 3a, a Pd atom bond with two oxygen atoms of TiO₂ surface; the Pd atom in Figure 3a is highly unstable. Compared to the structure in Figure 3a, we find that one or two oxygen atoms (O_{ad}) can be added between Pd_i and one 5-coordinated Ti atoms (Ti_{5c}) near to the Pd_i atom, forming a different structure (Figures 3b) in which three O atoms coordinate with the Pd atom. Adding two oxygen atoms between Pd_i and two Ti_{5c} can form two different structures (Figures 3c and 3d) in which four oxygen atoms bond with a Pt atom. The structure in Figure 3c is more stable than the one in Figure 3b by about 30 kJ/mol. Table S3 lists the calculated formation energy of oxygen adatoms for structures in Figure 3. The structural

optimization with DFT shows that the average Pd-O distance in structure of Figure 3c is 2.06 Å, in good agreement with the experimental values, 2.00 Å measured with EXAFS (Figure 2e). As shown in Table 1 in Supporting Information, formation of this structure (Figure 3c) is highly energetically favorable with an energy gain of 128 kJ/mol. Although structure of Figure 3d has a Pd atom coordinating with four oxygen atoms (Pd_iO₄), it has definitely higher energy than Figure 3c. Thus, Figure 3d is not a favorable structure. As the coordination number of O atoms to a Pd atom and the optimized distance between Pd and O in the structure of Figure 3c are quite consistent with the measured values of catalyst 0.20 wt% Pd/TiO₂ (Figure 2f), we take the structure in Figure 3c as active site of Pd_i/TiO₂ in the following simulation of reaction pathway of C-C coupling reaction on Pd_i/TiO₂.

Our DFT calculations suggested that the C-C coupling performs on Pd_i/TiO₂ through four steps on a Pd-O_{ad}-Ti_{5c} site (Figure 3f). In the first step iodobenzene adsorbs on the anchored Pd_i atom with an adsorption energy of 56 kJ/mol (Figure 3f-I) and then C-I bond is broken (Figure 3f-III). Then, the iodine atom adsorbs on the adjacent Ti_{5c} atom with an apparent barrier of 40 kJ/mol (Figure 3f-II) referenced to the energy of gas phase iodobenzene. The remaining phenyl group binds to the Pd atom (Figure 3f-III). The second step is physisorption of phenylacetylene molecule (Figure 3f-IV). The third step is the dissociative adsorption of C-H bond of phenylacetylene. The C-H bond of acetylenyl of HC≡C-C₆H₅ interacts with O_{ad} of TiO₂, resulting in breakage of this C-H bond (Figure 3f-V); this is due to the nature of high activity of the O_{ad} atom. Upon this dissociation, phenylacetylenyl binds to the O_{ad} atom; the H atom couples with adsorbed iodine atom, forming HI which is one product. The fourth step is the interaction between the adsorbed C₆H₅ and C₆H₅C≡C through the transition state (Figure 3f-VI) to form product molecule C₆H₅-C≡C-C₆H₅.

As shown in the energy profile (Figure 3f), the step of dehydrogenation of phenylacetylene (from IV to V in Figure 3f) is barrier-less and highly exothermic with a large energy gain of 170 kJ/mol. The last step is the coupling between the phenyl group adsorbed on the Pd atom and the phenylacetylenyl bound on the O_{ad} site due to their close proximity as shown in Figure 3f-V. Although this step has an activation barrier of 72 kJ/mol, the gained energy, 170 kJ/mol in the C-H dissociation of phenylacetylene (from IV to V) makes the intermediate (Figure 3f-V) have enough energy to cross the barrier of 72 kJ/mol for coupling between phenyl and phenylacetylenyl (Figure 3f-VI). Thus, we can consider that the step from adsorption of phenylacetylene (Figure 3f-IV) to formation of product diphenylacetylene (Figure 3f-VII) is barrierless. From this point of view, the rate-limiting step of this pathway is thus the dissociative chemisorption of iodobenzene; activation barrier of this step is 52 kJ/mol (Figure 3f-II) if referenced to energy of gaseous iodobenzene (the black dashed line aligned to 0 kJ/mol). It agrees reasonably with the experimental value derived from the Arrhenius plot of kinetics studies of C-C coupling on Pd_i/TiO₂, 28.9 kJ/mol (Figure 4d). This difference between the calculated value

and the experimental one likely results from the solvent effect that was not included in the computational studies. It is expected that the solvent could lower the activation barrier by stabilizing the transition state (structure II in Figure 3). In summary, the theoretical simulation of C-C coupling on Pd_i/TiO₂ suggested that the unique site Pd-O_{ad}-Ti_{5c} provides multifunctional atoms Pd, O_{ad}, and Ti_{5c} for activating C-I of iodobenzene, activating C-H of phenylacetylene and then performing C-C coupling to form diphenylacetylene.

SUMMARY

We have shown for the first time the efficient C-C coupling on single atom sites anchored on an oxide support. Spectroscopic evidence confirmed the preservation of single Pd atom (Pd_iO₄) sites anchored on TiO₂ of used catalyst after catalysis. This single-atom catalyst exhibits high activity and selectivity. Systematic control experiments confirmed the durability of these single atoms sites anchored to TiO₂. Kinetic studies show that the apparent activation barrier of C-C coupling on Pd_i/TiO₂, 28.9 kJ/mol is lower than 51.7 kJ/mol on molecular catalyst Pd(PPh₃)₂Cl₂. Computational studies suggest that Pd atom anchored to four oxygen atoms of TiO₂ through Pd-O-Ti bonds is a thermodynamically favorable structure. A catalytic cycle was proposed, in which the rate-determining step is the dissociative chemisorption of iodobenzene with an activation barrier of this step is 40 kJ/mol. This activation barrier agrees basically with the experimental value (28.9 kJ/mol) derived from the Arrhenius plot of kinetics studies of C-C coupling on Pd_i/TiO₂. The high activity and selectivity of C-C coupling on single Pd atom sites anchored on TiO₂ suggest a new chemical route to perform C-C coupling which are mostly catalyzed by Pd-based molecular catalysts; in this route products can be readily separated from catalyst.

Supporting Information. Computational studies, control experiment for checking whether Pd atoms of 0.20 wt% Pd/TiO₂ detached or not, catalytic activity for C-C coupling on Pd_i/TiO₂ in solvent benzene, computational studies. This material is available free of charge via the Internet at <http://pubs.acs.org>.

AUTHOR INFORMATION

Corresponding Author

* To whom all correspondence should be addressed.
Email: franklin.feng.tao@ku.edu

Funding Sources

This work was supported by Chemical Sciences, Geosciences and Biosciences Division, Office of Basic Energy Sciences, Office of Science, U.S. Department of Energy.

ACKNOWLEDGMENT

This work was mainly supported by the U.S. Department of Energy, Office of Science, Office of Basic Energy Sciences, Chemical Sciences, Geosciences, and Biosciences Division under Award Number DE-SC0014561.

REFERENCES

1. Beletskaya, I. P.; Cheprakov, A. V. *Chem. Rev.* **2000**, *100* (8), 3009-3066.
2. Chinchilla, R.; Najera, C. *Chem. Rev.* **2007**, *107* (3), 874-922.
3. Li, Y. G.; Zhou, P.; Dai, Z. H.; Hu, Z. X.; Sun, P. P.; Bao, J. C. *New J. Chem.* **2006**, *30* (6), 832-837.
4. Son, S. U.; Jang, Y.; Park, J.; Na, H. B.; Park, H. M.; Yun, H. J.; Lee, J.; Hyeon, T. *J. Am. Chem. Soc.* **2004**, *126* (16), 5026-5027.
5. Thathagar, M. B.; Kooyman, P. J.; Boerleider, R.; Jansen, E.; Elsevier, C. J.; Rothenberg, G. *Adv. Synth. Catal.* **2005**, *347* (15), 1965-1968.
6. Hu, J.; Liu, Y. B. *Langmuir* **2005**, *21* (6), 2121-2123.
7. Kogan, V.; Aizenshtat, Z.; Popovitz-Biro, R.; Neumann, R. *Org. Lett.* **2002**, *4* (20), 3529-3532.
8. Moreno-Manas, M.; Pleixats, R. *Account. Chem. Res.* **2003**, *36* (8), 638-643.
9. Thathagar, M. B.; Beckers, J.; Rothenberg, G. *J. Am. Chem. Soc.* **2002**, *124* (40), 11858-11859.
10. Li, Y.; Boone, E.; El-Sayed, M. A. *Langmuir* **2002**, *18* (12), 4921-4925.
11. Kim, S. W.; Kim, M.; Lee, W. Y.; Hyeon, T. *J. Am. Chem. Soc.* **2002**, *124* (26), 7642-7643.
12. De La Rosa, M. A.; Velarde, E.; Guzmán, A. *Syn. Commun.* **1990**, *20* (13), 2059-2064.
13. Kaneda, K.; Higuchi, M.; Imanaka, T. *J. Mol. Catal.* **1990**, *63* (3), L33-L36.
14. Marck, G.; Villiger, A.; Buchecker, R. *Tetrahedron Lett.* **1994**, *35* (20), 3277-3280.
15. Miyaura, N.; Suzuki, A. *Chem. Rev.* **1995**, *95* (7), 2457-2483.
16. Roth, G. P.; Farina, V.; Liebeskind, L. S.; Peña-Cabrera, E. *Tetrahedron Lett.* **1995**, *36* (13), 2191-2194.
17. Kang, S.-K.; Lee, H.-W.; Jang, S.-B.; Kim, T.-H.; Kim, J.-S. *Syn. Commun.* **1996**, *26* (23), 4311-4318.
18. Suzuki, A. *J. Organomet. Chem.* **1999**, *576*

- (1), 147-168.
19. Welton, T. *Chem. Rev.* **1999**, *99* (8), 2071-2084.
20. Biffis, A.; Zecca, M.; Basato, M. *J. Mol. Catal. A: Chem.* **2001**, *173* (1), 249-274.
21. Littke, A. F.; Fu, G. C. *Angew. Chem. Int. Ed.* **2002**, *41* (22), 4176-4211.
22. Yin, L.; Liebscher, J. *Chem. Rev.* **2007**, *107* (1), 133-173.
23. Li, Y.; Fan, X. B.; Qi, J. J.; Ji, J. Y.; Wang, S. L.; Zhang, G. L.; Zhang, F. B. *Nano Res.* **2010**, *3* (6), 429-437.
24. Stevens, P. D.; Li, G.; Fan, J.; Yen, M.; Gao, Y. *Chem. Commun.* **2005**, (35), 4435-4437.
25. Cao, S. W.; Tao, F.; Tang, Y.; Li, Y. T.; Yu, J. G. *Chem. Soc. Rev.* **2016**, *45* (17), 4747-4765.
26. Bratlie, K. M.; Lee, H.; Komvopoulos, K.; Yang, P. D.; Somorjai, G. A. *Nano Lett.* **2007**, *7* (10), 3097-3101.
27. Joo, S. H.; Park, J. Y.; Renzas, J. R.; Butcher, D. R.; Huang, W. Y.; Somorjai, G. A. *Nano Lett.* **2010**, *10* (7), 2709-2713.
28. Kresse, G.; Furthmuller, J. *Phys. Rev. B* **1996**, *54* (16), 11169-11186.
29. Perdew, J. P.; Burke, K.; Ernzerhof, M. *Phys. Rev. Lett.* **1996**, *77* (18), 3865-3868.
30. Blöchl, P. E. *Phys. Rev. B* **1994**, *50* (24), 17953-17979.
31. Kresse, G.; Joubert, D. *Phys. Rev. B* **1999**, *59* (3), 1758-1775.
32. Grimme, S.; Antony, J.; Ehrlich, S.; Krieg, H. *J. Chem. Phys.* **2010**, *132* (15), 154104.
33. Henkelman, G.; Uberuaga, B. P.; Jonsson, H. *J. Chem. Phys.* **2000**, *113* (22), 9901-9904.
34. Henkelman, G.; Jonsson, H. *J. Chem. Phys.* **2000**, *113* (22), 9978-9985.
35. Howard, C. J.; Sabine, T. M.; Dickson, F. *Acta Crystallogr. B* **1991**, *47*, 462-468.
36. Mery, D.; Heuze, K.; Astruc, D. *Chem. Commun.* **2003**, (15), 1934-1935.
37. Leadbeater, N. E.; Tominack, B. J. *Tetrahedron Lett.* **2003**, *44* (48), 8653-8656.
38. Király, Z.; Dékány, I.; Mastalir, Á.; Bartók, M. *J. Catal.* **1996**, *161* (1), 401-408.
39. Ayyappan, S.; Gopalan, R. S.; Subbanna, G.; Rao, C. J. *Mater. Res.* **1997**, *12* (02), 398-401.
40. Sarkany, A.; Papp, Z.; Sajó, I.; Schay, Z. *Solid State Ionics* **2005**, *176* (1), 209-215.
41. Burton, P. D.; Boyle, T. J.; Datye, A. K. *J. Catal.* **2011**, *280* (2), 145-149.

TABLE OF CONTENT

